

TITLE PAGE

Citation Format:

G. Maffeis, A. Pifferi, A. Dalla Mora, L. Di Sieno, R. Cubeddu, A. Tosi, E. Conca, A. Giudice, A. Ruggeri, S. Tisa, A. Flocke, B. Rosinski, J.-M Dinten, M. Perriollat, C. Frascini, J. Lavaud, S. Arridge, G. Di Sciacca, A. Farina, P. Panizza, E. Venturini, P. Gordebeke, Paola Taroni, "Breast lesion classification based on absorption and composition parameters: a look at SOLUS first outcomes," Proc. SPIE 12376, Optical Tomography and Spectroscopy of Tissue XV, 123760K (7 March 2023);

Copyright notice:

Optical Tomography and Spectroscopy of Tissue XV, edited by Sergio Fantini, Paola Taroni, Proc. of SPIE Vol. 12376, 123760K · © 2023 SPIE

DOI abstract link:

<https://doi.org/10.1117/12.2648945>

Breast lesion classification based on absorption and composition parameters: a look at SOLUS first outcomes

G. Maffei^{*a}, A. Pifferi^a, A. Dalla Mora^a, L. Di Sieno^a, R. Cubeddu^a, A. Tosi^b, E. Conca^b, A. Giudice^c, A. Ruggeri^c, S. Tisa^c, A. Flocke^d, B. Rosinski^e, J.-M. Dinten^f, M. Perriollat^f, C. Frascini^g, J. Lavaud^g, S. Arridge^h, G. Di Sciacca^h, A. Farinaⁱ, P. Panizza^j, E. Venturini^j, P. Gordebeke^k, P. Taroni^a

^aPolitecnico di Milano - Dipartimento di Fisica, Piazza Leonardo da Vinci 32, 20133 Milano (Italy); ^bPolitecnico di Milano - Dipartimento di Elettronica, Informazione e Bioingegneria, Piazza Leonardo da Vinci 32, 20133 Milano (Italy);

^cMicro Photon Devices Srl, Via Waltraud Gebert Deeg 3F, 39100 Bolzano (Italy); ^dC-Haus, Am Kuemmerling 18, 55294 Bodenheim (Germany); ^eVermon SA, 180 Rue du Général Renault, 37000, Tours (France); ^fCEA-LETI, 17 Avenue des Martyrs, 38054 Grenoble (France); ^gHologic Supersonic Imagine, S.A., 510 rue René Descartes, 13857 Aix en Provence (France); ^hUniversity College London, Department of Computer Science, Gower Street WC1E 6BT London (UK); ⁱConsiglio Nazionale delle Ricerche, Istituto di Fotonica e Nanotecnologie, Piazza Leonardo da Vinci 32, 20133 Milano (Italy); ^jScientific Institute (IRCCS) Ospedale S. Raffaele-Breast Imaging Unit, Via Olgettina 60, 20132 Milano (Italy); ^kEuropean Institute for Biomedical Imaging Research, Am Gestade 1, 1010, Vienna (Austria)

ABSTRACT

A machine learning classification algorithm is applied to the SOLUS database to discriminate benign and malignant breast lesions, based on absorption and composition properties retrieved through diffuse optical tomography. The Mann-Whitney test indicates oxy-hemoglobin (p-value = 0.0007) and lipids (0.0387) as the most significant constituents for lesion classification, but work is in progress for further analysis. Together with sensitivity (91%), specificity (75%) and the Area Under the ROC Curve (0.83), special metrics for imbalanced datasets (27% of malignant lesions) are applied to the machine learning outcome: balanced accuracy (83%) and Matthews Correlation Coefficient (0.65). The initial results underline the promising informative content of optical data.

Keywords: Breast cancer, diffuse optical tomography, breast composition, lesion classification, machine learning, diffuse optics, time domain

1. INTRODUCTION

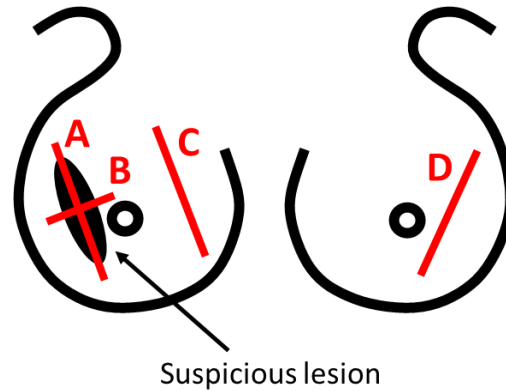
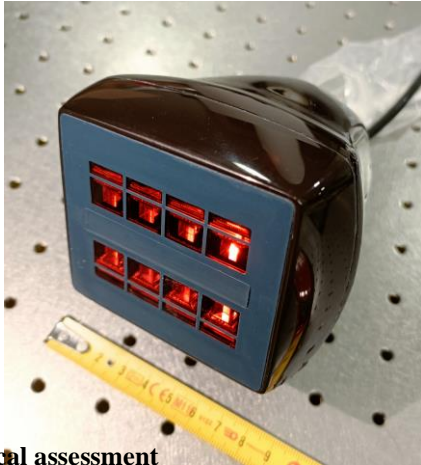
SOLUS stands for “Smart Optical and UltraSound device for the diagnostics of breast cancer” [1]. The name itself suggests the purpose and the methods of the H2020 EU-funded project (grant n° 731877): improving the diagnosis of the most widespread female carcinoma with a novel multimodal probe. More in details, SOLUS aims at discriminating benign and malignant breast lesions non-invasively as to reduce unnecessary biopsies.

The project included the design, development and testing in clinics of the device. Even if the project is finished, the feasibility study is going on and the richer and richer database allows for an initial breast composition estimation and a preliminary application of machine learning algorithms for lesions classification, as presented in this work.

2. MATERIALS AND METHODS

2.1 Instrument

SOLUS is a multimodal device that combines time-resolved multiple wavelength diffuse optical tomography (DOT, tissue composition), B-mode ultrasounds (US, morphology), color doppler (CD, vascularization) and shear wave elastography (SWE, stiffness) in a unique hand-held probe. While the ultrasound transducer is commercial (Aixplorer Mach 30 by Hologic SuperSonic Imagine S.A.), the 8 smart optodes are the break-through technology introduced by SOLUS itself (*i.e.*, the first miniaturization of time domain multi-wavelength diffuse optics). Each of them is a stand-alone module including 8 picosecond pulsed lasers (640, 675, 830, 905, 930, 970, 1020, 1050 nm), a large area fast-gated digital SiPM detector with integrated Time-to-Digital converter (Fig. 1) [2].



2.2 Clinical assessment

Figure 1 (Left) The SOL-US probe. Each red window corresponds to an optode, the central component is the US transducer. The clinical validation envisions the enrollment of 40 patients, 20 with malignant and 20 with benign lesions, who signed a written informed consent. The SOL-US acquisition is a progression of B-mode US, CD, SWE and DOT images. For each patient, the sequence is repeated in 4 different locations: on the lesion main axis (A), orthogonally to the previous orientation (B), far from the lesion of the same breast (C) and controlaterally in the mirrored position (D), as depicted in Fig. 2, to estimate the contrast between lesion and healthy tissue more reliably. Also, the measurement is performed by 3 radiologists with diverse experience, in order to assess reproducibility. Hence, each patient undergoes a total of 12 acquisitions in about one hour. So far, 22 lesions (6 malignant and 16 benign) have been examined.

2.3 Optical tomography

The following preliminary analysis is limited to US-guided optical data only. In fact, from the US B-mode image, a lesion segmentation is obtained and extrapolated to 3D to be used as morphological prior for the optical reconstruction [3]. DOT reconstructions exploit the Born approximation of the heterogenous analytical solution of the diffusion equation to estimate the absorption coefficients of the investigated breast tissue at the 8 wavelengths [4]. The breast tissue composition (oxy- and deoxy-hemoglobin, water, lipids, and collagen concentrations) is later retrieved by applying the Lambert-Beer law. The heterogenous model is based on the contrast between the “perturbation” and the background, thus it needs to couple one acquisition on the lesion (A, B) and one on the healthy tissue (C, D), for a total of 4 possible combinations. Mean values for constituent concentrations have been derived by averaging separately inside and outside the region of interest defined by the 3D extrapolation from the segmentation. In this work, we will focus on the lesion’s properties only.

2.4 Lesion classification

A KNN supervised machine learning algorithm (K-nearest neighbors, $K=1$) has been applied to classify benign and malignant lesions. 13 predictors have been selected (absorption coefficients at the 8 wavelengths and the 5 investigated constituents), by using 80% of the samples for training and 20% for testing. At this stage, the 12 results (4 combinations for 3 radiologists) available for each patient have been considered as independent. This is not rigorously true, but still it is an initial practical approach to increase the database size and help statistical relevance. Together with this disclaimer, another remark needs special attention: the dataset is imbalanced, as only the 27% of lesions is malignant. Consequently, together with standard indexes such as sensitivity, specificity and the Area Under the Curve (AUC) of the Receiver Operating Characteristic (ROC), special metrics adequate for imbalanced datasets are applied, such as the balanced accuracy and the Matthews Correlation Coefficient (MCC), that represent the fair counterpart of accuracy and F1 score, respectively [5]. Compact definitions are reported in Table 1, but a brief description of each metrics follows:

- Sensitivity [0, 1]: percentage of true cases correctly recognized as such.

- Specificity [0, 1]: percentage of false cases correctly recognized as such.
- AUC of ROC [0, 1]: since the ROC curve plots True Positive Rate vs False Positive Rate at different thresholds, the AUC represents the probability that the classification model positions a random positive example higher than a random negative one.
- Accuracy [0, 1]: fraction of correct predictions.
- Balanced accuracy [0, 1]: normalized fraction of correct predictions.
- F1 score [0, 1]: harmonic mean of precision (*i.e.*, the probability to be really positive, in case of a positive test result) and recall (equivalent to sensitivity). It is noticeable from the formula in Table 1 that negative cases are not considered.
- MCC [-1, +1]: measure of informedness (*i.e.*, quantification of how informed is the model about negative and positive cases) and markedness (*i.e.*, quantification of trustworthiness of negative and positive predictions), the unbiased counterparts of precision and recall, respectively.

Finally, the Mann-Whitney U test has been applied to verify the significance of the difference between benign and malignant populations for each of the 13 parameters [6].

3. RESULTS AND DISCUSSION

As regards the constituents' concentrations, the Mann-Whitney U test reveals that so far oxy-hemoglobin and lipids, in this order, are the most significant parameters for lesion classification (p-value respectively equal to 0.0007 and 0.0387). This could be due to the fact that in some cases the estimate of deoxy-hemoglobin, water and collagen gives null values with the standard approach to data analysis (estimate of absorption, followed by Lambert-Beer law to estimate tissue composition). Based also on the results of our previous studies, a spectrally constrained global approach [7], where the Lambert-Beer law is directly replaced in the diffusion equation, will be applied in the future aiming at a more robust data interpretation.

The sensitivity and specificity obtained based on the results of the machine learning algorithm are respectively 91% and 75%, while the AUC under the ROC curve is 0.83. The balanced accuracy is 83%, against 87% of the standard one. Moreover, the MCC value is equal to 0.65, against the F1 score which is 0.91. The metrics specific for imbalanced datasets (balanced accuracy and MCC) are lower than the equivalent standard measures, but still the outcomes underline the promising informative content of optical data.

Table 1. Metrics definition. TP = true positive, FN = false negative, TN = true negative, FP = false positive, TPR = TP/(TP+FN) true positive rate, TNR = TN/(TN+FP) true negative rate, FPR = FP/(FP+TN) false positive rate.

Sensitivity	$\frac{TP}{TP + FN} = 0.91$	Specificity	$\frac{TN}{TN + FP} = 0.75$
Accuracy	$\frac{TP + TN}{TP + TN + FP + FN} = 0.87$	Balanced accuracy	$\frac{TPR + TNR}{2} = 0.83$
F1 score	$\frac{2TP}{2TP + FP + FN} = 0.91$	MCC	$\frac{TP TN - FP FN}{\sqrt{(TP + FP)(TP + FN)(TN + FP)(TN + FN)}} = 0.65$

4. CONCLUSION

In this work, we have presented an initial breast lesion classification into benign and malignant categories through machine learning and the Mann-Whitney U test applied to optically derived tissue absorption and composition. Results are promising and we plan to further develop data analysis by including CD, SWE and testing a spectrally constrained global approach. In the meantime, the clinical trial is going on, thus enriching the dataset.

ACKNOWLEDGMENTS

This project has received fundings from the European Union's Horizon 2020 research and innovation programme under grant agreement n° 731877. The project is an initiative of the Photonics Public Private Partnership.

REFERENCES

- [1] "SOLUS - Smart Optical and Ultrasound Diagnostics of Breast Cancer.", H2020 Proj. grant No. 731877, <<http://www.solus-project.eu/>>.
- [2] Conca, E., Sesta, V., Buttafava, M., Villa, F., Di Sieno, L., Dalla Mora, A., Contini, D., Taroni, P., Torricelli, A., Pifferi, A., Zappa, F. and Tosi, A., "Large-Area, Fast-Gated Digital SiPM With Integrated TDC for Portable and Wearable Time-Domain NIRS," *IEEE J. Solid-State Circuits* **55**(11), 3097–3111 (2020).
- [3] Di Sciacca, G., Di Sieno, L., Farina, A., Lanka, P., Venturini, E., Panizza, P., Dalla Mora, A., Pifferi, A., Taroni, P. and Arridge, S. R., "Enhanced diffuse optical tomographic reconstruction using concurrent ultrasound information," *Philos. Trans. R. Soc. A Math. Phys. Eng. Sci.* **379**(2204), 20200195 (2021).
- [4] Di Sciacca, G., Maffei, G., Farina, A., Dalla Mora, A., Pifferi, A., Taroni, P. and Arridge, S., "Evaluation of a pipeline for simulation, reconstruction, and classification in ultrasound-aided diffuse optical tomography of breast tumors," *J. Biomed. Opt.* **27**(03), 1–19 (2022).
- [5] Chicco, D. and Jurman, G., "The advantages of the Matthews correlation coefficient (MCC) over F1 score and accuracy in binary classification evaluation," *BMC Genomics* **21**(1), 6 (2020).
- [6] McKnight, P. E. and Najab, J., "Mann-Whitney U Test," [The Corsini Encyclopedia of Psychology], John Wiley & Sons, Inc., Hoboken, NJ, USA, 531–594 (2010).
- [7] D'Andrea, C., Spinelli, L., Bassi, A., Giusto, A., Contini, D., Swartling, J., Torricelli, A. and Cubeddu, R., "Time-resolved spectrally constrained method for the quantification of chromophore concentrations and scattering parameters in diffusing media," *Opt. Express* **14**(5), 1888 (2006).